SEMPA IMAGING OF DOMAIN DYNAMICS IN AMORPHOUS METALS

A. Gavrin

Indiana University-Purdue University Indianapolis, Dept. of Physics, 402 N. Blackford St., Indianapolis, IN 46202.

J. Unguris

Electron Physics Group, National Institute of Standards and Technology, Gaithersburg, MD 20899-8412.

We show how Scanning Electron Microscopy with Polarization Analysis (SEMPA) may be used to observe domain wall motion in amorphous ferromagnetic ribbons commonly used in transformer cores. SEMPA images were obtained from both the smooth, air side of the ribbon, as well as the rough, difficult to image, wheel side. Domain wall motion was studied under both quasi-static and low frequency fields (4 Hz). The domain walls are observed to have a wide range of mobilities and are occasionally pinned by surface defects even in well annealed samples. Irreproducible domain wall motion was also observed, but was not always obviously related to defects. This has significant implications for future attempts to use stroboscopic measurements in the study of wall mobility at higher frequencies.

Introduction

Domain wall motion in magnetic materials is a critical aspect of the performance of many devices.[1] Power line transformers, inductor cores, magnetic field sensors, and recording heads all rely on the motion of magnetic domain walls over a wide frequency range. The primary goal of this work was to investigate the feasibility of applying Scanning Electron Microscopy with Polarization Analysis (SEMPA)[2] to the study of domain wall motion. We chose to study amorphous metal samples because the unique ability of SEMPA to separate magnetic and topographic information is useful in correlating the magnetization dynamics of these materials with their physical structure.

Optimizing the magnetic properties of an amorphous metal depends strongly on controlling the physical structure. We investigated field annealed METGLAS™ Transformer Core Alloy (TCA) ribbons provided by AlliedSignal Inc[3]. This material is an amorphous alloy of the Fe-Si-B family that is produced for use in power distribution transformers.[4] It is well known that to minimize losses in a transformer the core must be magnetically soft and have high resistivity. In addition, to further reduce eddy current losses, it is desirable that the core domain structure con-

sists of a large number of narrow, parallel domains.[5] Thus, each wall moves only a short distance during each magnetization cycle. This condition, known as domain refinement, has been achieved in Fe-Si transformer steels by mechanical scratching and by laser scribing of the laminates before the final core is constructed.[6]

In amorphous transformer cores the desired domain structure is induced when the core is annealed under an applied field. This process relieves strains that are quenched into the material during casting, and introduces magnetocrystalline anisotropy parallel to the field due to pair correlations produced by diffusion during the anneal.[7] In addition, it is believed that some surface imperfections created during the casting process help to nucleate domains, further increasing their numbers.

SEMPA offers two features that are especially useful in analyzing the magnetic microstructure of amorphous ribbons: First, the magnetization and topographic images are acquired simultaneously and independently making the investigation of correlations between magnetic and physical structure straight forward. Second, the electron microscope's large depth of field makes imaging rough surfaces possible. These features allowed us to study the domain structures on both surfaces of the ribbons. **Figure 1** shows an example of a SEMPA image from the smoother, air side of a ribbon. **Figure 2** shows a SEMPA image from the side of the ribbon that forms against the wheel during the spin casting process. The wheel side is far rougher, exhibiting a variety of deep pits, scratches and other defects, but SEMPA is still able to image the magnetic structure. The images in these examples are from an as cast ribbon. The complex domain structure is dominated by magnetoelestic effects. The rest of this paper will deal with annealed ribbons, in which the complexity of the domain structures is greatly reduced.

In this paper, we will describe our application of SEMPA to the study of domain wall motion in amorphous metals. We will present our studies of domain wall motion under quasi-static conditions and at frequencies up to 4 Hz. Of particular interest was the reproducibility of the domain wall motion, since extending SEMPA imaging to higher frequencies will probably involve using stroboscopic methods.

Sample Preparation

Because SEMPA is an electron microscope based technique, imaging cannot easily be carried out with a large external magnetic field present at the sample surface. Therefore, in order to measure the domain dynamics, a closed loop magnetic circuit configuration was used. Rectangular samples 4 mm wide by 40 mm long were cut from the center of a 20 cm wide ribbon, with the long axis of the sample parallel to the original ribbon axis. The samples were then mounted in a sample holder shown schematically in **Fig. 3.** The ribbon passed through primary (drive) coils and secondary (pickup) coils, and the ends were tightly clamped together. A top plate (not shown) with a beveled hole held the segment of the ribbon exposed to the electron beam flat, while allowing access for secondary electron extraction. This closed loop configuration kept the interaction between the applied field and the incident and scattered electrons to a minimum. At drive coil currents sufficient to saturate the sample, the fringe field two mm from the sample was

less than 0.1 Oe. This field did not measurably affect the incident electron beam, and only produced a 2% change in the intensity of the secondary electrons at the detector. Samples were cleaned *in situ* for SEMPA imaging by ion sputtering with 2 keV Ar ions. The samples were not annealed after sputtering.

Samples of METGLAS™ TCA were obtained from AlliedSignal corporation in the form of 20 cm wide melt-spun ribbons. These materials were investigated in both the as cast state and after annealing under a magnetic field applied along the ribbon axis. During the anneal, the sample was held at 350 °C for 1.5 hours, cooled at 2 °C/min to 200 °C, then cooled to room temperature overnight. The entire process was carried out under an applied field of 1.2×10^{-3} T in an argon atmosphere. The rest of the images in this paper are from the air side of the annealed ribbon.

These annealing procedures have been shown to produce the optimum domain structure for transformer core applications.[8] The field anneal imparts a uniaxial anisotropy along the long direction of the ribbon. This anisotropy induces a domain configuration consisting of many long domains parallel to the ribbon axis. This configuration was verified in SEMPA measurements at zero applied field. When placed in the sample holder as shown in **Fig. 3**, a drive signal applied at the primary coil causes the domain walls to move in the transverse direction. This magnetization signal may be observed at the secondary coils as well as by SEMPA imaging of the domains.

SEMPA Measurements

Domain wall motion was investigated under two conditions: quasi-static and low frequency sinusoidal. In the quasi-static mode a constant magnetic field was applied to the sample by passing a DC current through the primary coil, and the static magnetic domain pattern was recorded. The current was then incremented and SEMPA images were acquired over a complete hysteresis cycle.

Four domain images from various parts of a quasi-static magnetization cycle are displayed in **Fig. 4a-d**; the images are keyed to the hysteresis loop shown in **Fig. 4e**, which was acquired at 50 Hz, and is shown only to illustrate the magnetization state in each of the four images. These images were taken in the vicinity of a surface defect (shown in **Fig. 4f**), which pins the domain walls. Sequences such as that shown in **Fig. 4** were recorded in areas without defects as well.

In the second mode, the SEMPA image was acquired while a low frequency oscillating current was applied to the drive coil. This method is similar to that used by J. D. Livingston, et al., with Type II contrast SEM domain imaging.[9] The frequency of the drive current was selected such that its period was longer than the time required to scan one line of the image and less than the time required to acquire an image. The maximum frequency is therefore determined by the minimum dwell time per pixel, which, for our instrumentation, was about 1 msec. At 128 pixels per line our maximum frequency is about 8 cycles per second. Our typical high resolution images are 256 columns by 192 rows of pixels with a 1 msec dwell. In this case a 1 Hz drive current frequency results in about 4 lines per period. In such images, the amplitude of the domain wall mo-

tion, the domain wall mobility, as a function of position on the sample is captured in a single image.

Representative examples of low frequency images are shown in **Fig. 5**. The figure shows the motion of the same pair of domain walls when AC fields of two different amplitudes are applied. In these images only the magnetization component along the ribbon's easy axis is shown. A zero applied field image is also included for reference.

Discussion

Low frequency images such as those shown in **Fig. 5** clearly demonstrate that the domain walls in our samples have widely varying mobilities. Even limiting our discussion to these long, straight walls, the amplitude of the domain wall motion varies by at least a factor of 4. The quasi-static images, such as those shown in **Fig. 4**, reveal that even in a well annealed sample some domain walls remained pinned by defects. Of course, the mobility of these walls is quite small.

Our observations under quasi-static conditions also revealed that some domain wall motions are not reproducible. This is illustrated in **Fig. 6** where we compare two SEMPA images that were obtained at the same applied field (near to saturation). The sample was taken through one complete hysteresis cycle between the two images. The difference between these two images is shown in **Fig. 6c**. Two distinct types of irreproducible behavior are shown in this example. First, the locations of the long domain walls are not reproduced exactly upon each return to saturation. One wall appears to return to the same position, the other does not. Second, the nuclei of reversed domains appear at different locations on the ribbon.

Irreproducible behavior was also observed in low frequency images. Unlike the reproducible domain wall motion observed in **Fig. 5**, the domain motion in the region of the ribbon viewed in **Fig. 7**, shows varying degrees of irreproducibility depending on the amplitude of the applied AC field. For low amplitudes the sample is only driven through a minor magnetization loop with little hysteresis, so the domain motion shown in **Fig. 7(a)** is very reproducible. For larger amplitudes, near the coercive field of the sample, the domain motion is the most irreproducible. This is seen in **Fig. 7(b)**. Interpretation of this image is difficult because of hysteresis, but, in general, the remanent dark domain (negative magnetization) occurs at a different location each time the field reaches positive saturation. During some of the cycles, the domain was either completely annihilated or formed beyond the range of the image. When the amplitude is large enough to drive the ribbon into saturation, the wall motion, after taking into account hysteresis, becomes more reproducible, however some irreproducible behavior still remains.

Irreproducible motions were observed both in the ideal areas of the sample, and in the vicinity of domains which were pinned by defects. Although we examined several ideal, featureless regions and several with defects present, no systematic correlation between the irreproducibility and proximity to defects was observed. Further investigations will be required to determine whether defects have small but statistically significant effects.

The presence of irreproducible wall motions complicates efforts to study these systems at higher frequencies. Stroboscopic measurements are a natural choice to image domain dynamics

at power line frequencies and above, because of the relatively slow image acquisition rate in scanning systems such as SEMPA. However, stroboscopic imaging will only capture reproducible motions clearly. Irreproducible motions will produce a blurring of the domain structure or, at best, an appearance similar to a photograph with multiple exposures on a single negative.

Summary

By using a minimum stray field sample/magnet configuration we have been able to use SEMPA to image magnetic domain structures and domain wall dynamics in AlliedSignal METGLAS™ TCA ribbons. Domain wall motions were observed under both quasi-static and low frequency conditions. The domain structure of the field annealed ribbons consisted primarily of long, straight, domains parallel to the ribbon axis. These walls were relatively mobile, but were found to have widely varying mobilities. In addition, some domains pinned by remaining defects in the ribbon structure were also observed. Furthermore, some features of the domain wall motion were found to be irreproducible, especially at large field amplitudes, although this irreproducible wall motion was not obviously correlated with surface defects. This irreproducibility creates significant challenges to future stroboscopic measurements in these systems.

The authors thank Anatol Rabinkin for helpful discussions and for providing the samples. This work was supported in part by the National Research Council and by the Office of Naval Research.

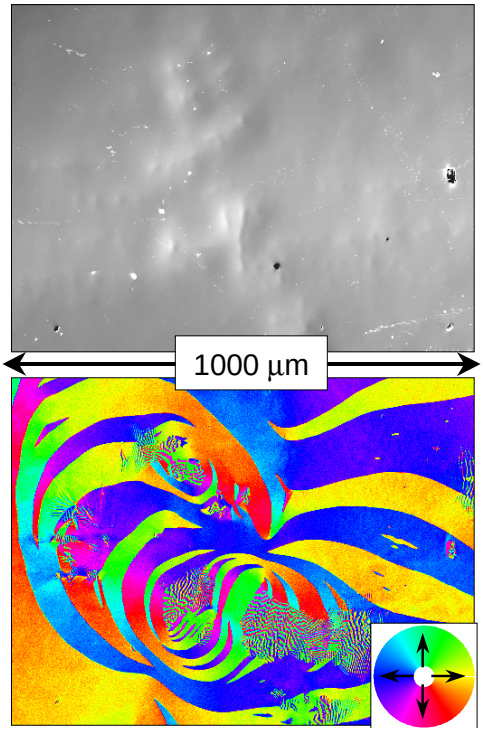

Fig.1 (above) SEMPA image of the magnetization direction (color) and topography from the air side of an as-cast amorphous ribbon. The magnetization direction is color coded to the color wheel in the inset. The ribbon's long axis is horizontal.

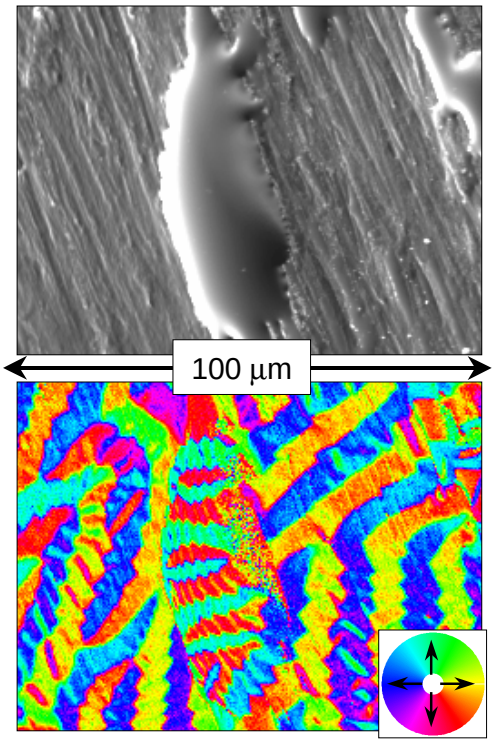

Fig. 2 (above) SEMPA image of magnetization and topography from the rough, wheel side of the same ribbon in Fig. 1.

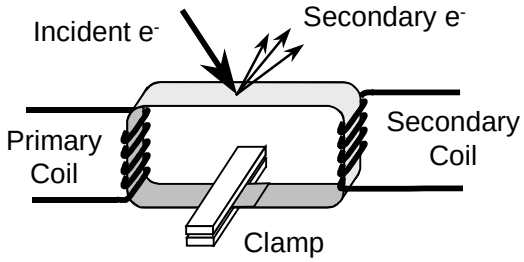

Fig. 3 (above) Sample holder schematic shows the closed loop ribbon sample and the magnetic circuit. The top aperture plate is not shown.

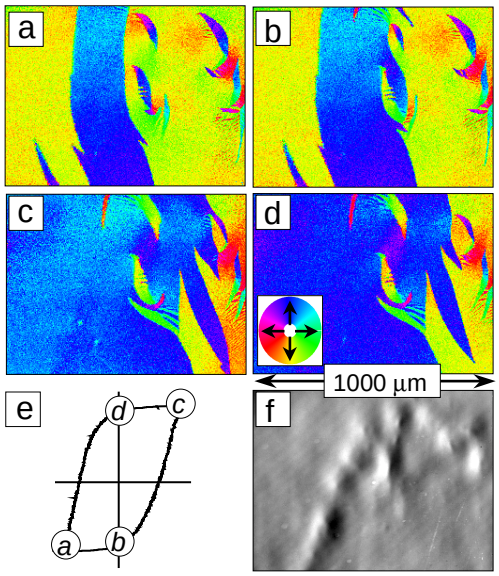

Fig. 4 (above) (a), (b), (c), and (d) are quasi-staic SEMPA images of the magnetization direction from various points along around the hysteresis curve shown in (e). The hysteresis curve was acquired at a higher frequency and is only representative of the true curve. Some of the domain walls are pinned by the defects shown in the topography image (f). The ribbon's long axis and the applied field direction is vertical in

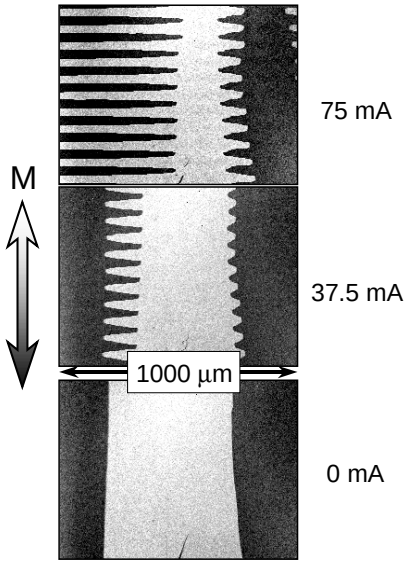

Fig. 5 (above) SEMPA images of a pair of domain walls acquired with an oscillating applied field present. Fields were generated by drive current amplitudes of 0, 37.5 mA and 75 mA . The ribbon's long axis is vertical in this image and only the magnetization component along this axis is shown.

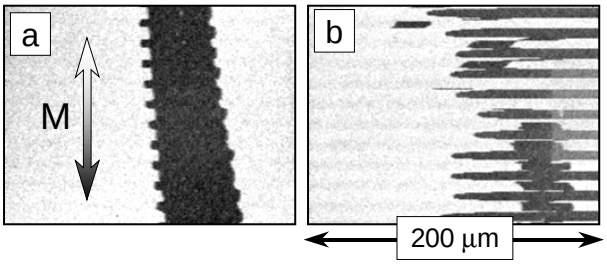

Fig. 7 (above) Irreproducible behavior of domain wall motion as a function of the amplitude of the applied field is shown in these SEMPA images with drive current amplitudes of (a) 25 mA and (b) 50 mA,

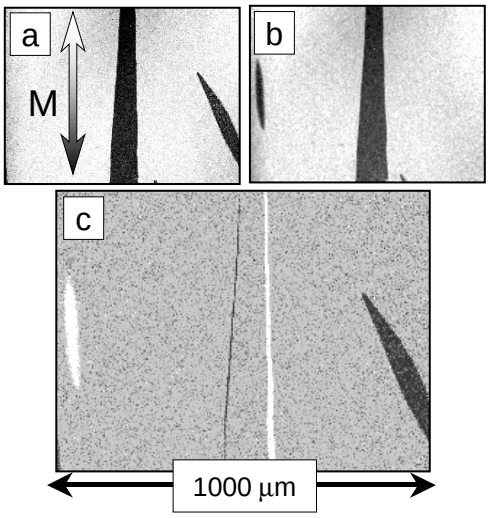

Fig. 6 (left) Irreproducibility of domains near saturation is shown by two SEMPA images, (a) and (b), taken at the same point in two consecutive hysteresis cycles. An enlarged view of the difference between these images is shown in (c). The difference image reveals irreproducible wall motion and domain nucleation. The ribbon's axis is vertical in this image and only the magnetization component along this axis is shown.

[1] A. H. Morrish, *The Physical Principles of Magnetism*, (Krieger, Malabar FL, 1983).

[2] M. R. Scheinfein, J. Unguris, M. H. Kelley, D. T. Pierce and R. J. Celotta, Rev. Sci. Instrum. **61**, 2501 (1990).

[3] Use of this material does not imply recommendation or endorsement by the National Institute of Standards and Technology, nor does it imply that the material is necessarily the best available for this purpose.

[4] C. H. Smith in *Rapidly Solidified Alloys: Processes, Structures, Properties and Applications*, (Marcel Dekker, New York, 1993).

[5] R. H. Pry and C. P. Bean, J. Appl. Phys. **29**, 532 (1958)

[6] T. Sato, K. Kuroki, and O. Tanaka, IEEE Trans. Mag. **MAG-14**, 350 (1978); T. Iuchi, S. Yamaguchi, T. Ichiyama, M. Nakamura, T. Ishimoto, and K. Kuroki, J. Appl. Phys. **53**, 2410 (1982).

[7] F. E. Luborsky and J. L. Walter, IEEE Trans. Mag. **MAG-13**, 953 (1977).

[8] H. Fujimori, H. Yoshimoto, T. Masumoto, and T. Mitera, J. Appl. Phys. 52, 1893 (1982); J. S. Song, H. B. Im, and M. S. Yun, J. Appl. Phys. **69**, 5014 (1991)

[9] J. D. Livingston and W. D. Morris, IEEE Trans. Magn. MAG-17, 2624 (1981).